Multiscale Modeling and Experimental Study of CO_2 Absorption into Ionic Liquid Reverse Micelle

Wei Shi*, L. Hong*, V. A. Kusuma and D. P. Hopkinson*

*U.S. Department of Energy, National Energy Technology Laboratory, Puittsburgh, PA, 15236, USA
wei.shi@netl.doe.gov

ABSTRACT

In this work, we have used both atomistic simulations and device-scale modeling of our experimental data to investiagte CO2 absorption in ionic liquid reverse micelle (ILRM). The ILRM consisted of 1-butyl-3 methylimidazolium tetrafluoroborate ([bmim][BF_4]) ionic liquid (IL) as the micelle core, the benzylhexadecyldimethylammonium ($[BHD]^+$) chloride ($[Cl]^-$) was the cationic surfactant, and benzene was used as the continuous solvent phase in this study. The atomistic simulations show show that [bmim][BF_4] inside the RM diffuses 5−26 times faster than the neat IL, which is partly due to the fast particle diffusion for the ILRM nanodroplet (IL and surfactant) as a whole in benzene solvent compared with neat [bmim][BF_4] diffusion. Furthermore, atomistic simulations show that CO_2 molecules are absorbed in four different regions of the ILRM system, that is, (I) in the IL inner core, (II) in the [BHD]+ surfactant cation layer, (III) at the interface between the [BHD]+ surfactant cation layer and benzene solvent, and (IV) in the benzene solvent. The CO_2 solubility was found to decrease in the order II > III ~ IV > I, while the CO_2 diffusivity and permeability decrease in the following order: IV > III > II > I. Finally, by using a device-scale modeling of our experimental CO_2 absorption solubility data, it was found that apparent CO_2 mass transport in the ILRM could be one magnitude faster compared with CO_2 mass transport in the corresponding neat IL and surfactant.

Keywords: Atomistic simulation, device-scale modeling, CO_2 absorption, ionic liquid, reverse micelle

1 INTRODUCTION

Highly viscous solvents for gas absorption will lead to large pumping power requirement and large absorption/desorption tower, resulting in high capital cost. Ionic liquids (ILs) represent such examples even though ILs have been extensively studied for gas separation due to their favorable properties, such as negligible volatility and large CO_2 solubility. In additional to the high viscosity, ILs are typically hygroscopic due to strong anion-water interactions. This IL hygroscopicity implies that water must be removed before CO_2 is captured. Both the high viscosity and hygroscopicity degrade the efficiency and economics of carbon capture by using ILs. In order to overcome the above two drawbacks, we have recently investigated IL reverse micelle (RM) for CO_2 capture [1]. The nano size and consequently the large specific surface area for the ILRM nanodroplet (IL core and surfactant) will significantly help gas mass transport. Additionally, a hydrophobic oil is used as the solvent phase to minimize water permeation through the ILRM system, which may alleviate problems related to water absorption in ILs.

In this talk, we present both atomistic and device scale modeling to investigate CO_2 absorption in ILRM. The ILRM consisted of 1-butyl-3-methylimidazolium tetrafluoroborate ([bmim][BF_4]) IL as the micelle core, the benzylhexadecyldimethylammonium ($[BHD]^+$) chloride ($[Cl]^-$) was the cationic surfactant, and benzene as the continuous solvent phase. Both our atomistic simulations and experiments show that the IL inside the RM diffuses 5-26 times faster than the neat IL, which is partly due to the fast particle diffusion for the ILRM nanodroplet as a whole in the less viscous oil solvent. Simulations show that CO_2 molecules are absorbed in four different regions of the ILRM system, that is, (I) in the IL inner core, (II) in the $[BHD]^+$ surfactant cation layer, (III) at the interface between the $[BHD]^+$ surfactant cation layer and benzene solvent, and (IV) in the benzene solvent. The CO_2 solubility was found to decrease in the order II > III ~ IV > I, while the CO_2 diffusivity and permeability decrease in the following order: IV > III > II > I. By combing the device-scale modeling with the unsteady-state CO_2 absorption data obtained from our experimental Sievert's apparatus, it was found that the apparent CO_2 mass transport in the ILRM could be one magnitude faster compared with CO_2 mass transport in the corresponding neat IL and surfactant. This is partly due to the large specific area for the ILRM nano particle. Both our simulations and experiments show that the ILRM is a promising material for CO_2 capture applications.

2 SIMULATION DETAILS

2.1 Atomistic Simulations

The molecular structures for the $[bmim]^+$ cation, $[BF_4]^-$ anion, $[BHD]^+$ surfactant cation, $[Cl]^-$ surfactant anion, and benzene solvent are shown in Figure 1. The classical force field (FF) potential used to simulate the [bmim][BF_4] IL, [BHDC] surfactant, benzene solvent, CO_2, and the interactions between these molecules is given by

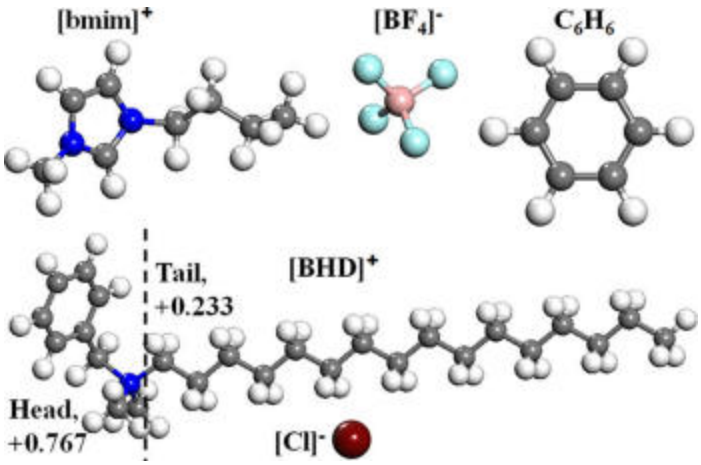

Figure 1. Molecular structures for 1-butyl-3-methylimidazolium cation ([bmim]$^+$), tetrafluoroborate anion ([BF_4]$^-$), benzylhexadecyldimethylammonium surfactant cation ([BHD]$^+$), chloride surfactant anion ([Cl]$^-$), and benzene (C_6H_6). A vertical dashed line was used to divide [BHD]+ into two groups, that is, the head group with a charge of +0.767 e and the alkyl chain tail group with a charge of +0.233 e. Note that the charges were obtained from quantum ab initio calculations of [BHD]$^+$ in the gas phase [1].

$$\begin{aligned}\mathcal{V}(r) = &\sum_{\text{bonds}} k_b(r - r_0)^2 + \sum_{\text{angles}} k_\theta(\theta - \theta_0)^2 \\ &+ \sum_{\text{dihedrals}} k_\chi[1 + \cos(n_0\chi - \delta_0)] \\ &+ \sum_{\text{impropers}} k_\psi(\psi - \psi_0)^2 \\ &+ \sum_{i=1}^{N-1}\sum_{j=i+1}^{N}\left\{4\varepsilon_{ij}\left[\left(\frac{\sigma_{ij}}{r_{ij}}\right)^{12} - \left(\frac{\sigma_{ij}}{r_{ij}}\right)^{6}\right] + \frac{q_i q_j}{r_{ij}}\right\}\end{aligned} \quad (1)$$

Standard Lorentz–Berthelot combining rules were used to calculate the mixed Lennard-Jones (LJ) interaction parameters. The LJ potential was switched from 10.5 to 12.0 Å. A Verlet neighbor list with a 13.5 Å radius was used. The intra molecular electrostatic and LJ interactions for atoms separated by exactly three consecutive bonds were scaled by 0.5 and were neglected for atoms separated by less than three consecutive bonds. The classical FF parameters for [bmim]+, [BF_4]- , and CO_2 were obtained from previous work[1].

2.2 Device Scale Modeling

CO_2 concentration in the liquid sample changes with time during the experimental CO_2 solubility measurement until an equilibrium is obtained. It is very important to note that stirring was not used in the experiment. The CO_2 mass transport in the liquid sample is completely due to CO_2 Fickian diffusion mechanism. By assuming 1-dimensional CO_2 Fickian diffusion along the Z-direction of the cylindrical tube containing the liquid sample, CO_2 concentration in the liquid sample was obtained as below

$$C(z,t) = Cs\left[1 - erf\left(\frac{z}{2\sqrt{Dt}}\right)\right] \quad (2),$$

where $C(z,t)$ is the CO_2 concentration in a unit of mol/liter at time t and position z, Cs is the CO_2 concentration at the top of the liquid surface (z=0). The *erf* is the mathematical error function, D is the CO_2 diffusivity in the liquid. Note that when deriving the equation (2), the following initial and boundary conditions were used: $C(z,0)=0$; and $C(0,t)=Cs$, $C(L,t)=0$, where L indicates the liquid thickness in the tube in Z direction; this boundary condition implies that Cs is a constant and there is no CO_2 absorbed at the bottom of the liquid sample in the tube. During CO_2 absorption experiment, after some time t_0, CO_2 will be diffused to the bottom of the tube and the above equation (2) will not be appropriate. But at $t < t_0$, $C(L,t)=0$ would hold. Consequently, only the experimental data at the initial time stage were used to fit equation (2). Additionally, at $t < t_0$, CO_2 pressure in the gas phase only slightly changes and Cs could be reasonably assumed to be a constant. For example, for CO_2 absorption in neat [bmim][BF_4] IL, only the CO_2 absorption experimental data at t < 36 minutes were used. During this time, CO_2 pressure in the gas phase only slightly decrease from 13.84 bar to 13.65 bar; the CO2 pressure in the gas phase and Cs for CO_2 could be reasonably assumed a constant. Additionally, at t < 36 minutes, CO_2 concentration at the bottom of the tube ($C(L,t)$) was calculated from equation (2) and was found to be negligibly small, very close to 0. Consequently, at t < 36 minutes, equation (2) would be appropriate to describe CO_2 concentrations in the IL sample. Note that in experiment the total number of CO_2 absorbed in the whole IL solvent sample, $N_{CO2}(t)$, instead of CO_2 concentrations at different IL position $C(z,t)$, was measured. In the modeling calculation, the $N_{CO2}(t)$ can be calculated from $C(z,t)$ by using the following integration equation,

$$N_{CO_2}(t) = \int_0^L A \times C(z,t)dz = Cs \times A\int_0^L \left[1 - erf\left(\frac{z}{2\sqrt{Dt}}\right)\right]dz \quad (3),$$

where A is the cross-section area for the tube ($\pi/4\times(18.98\text{mm})^2$). By tuning D and Cs, the $N_{CO2}(t)$ could calculated from (2) and compared with the experimental data. For CO_2 absorption in [bmim][BF_4], for the time period 2.95 min. ≤ t ≤ 35.95 min., there are totally 34 sets of experimental $N_{CO2}(t)$ data for comparison with the modeling. The folliwng minimization function was

consequently constructed,

$$obj = \sum_{i=1}^{34} N_{CO2}(\exp) - N_{CO2}(cal) = \int_0^L A \times C(z,t)dz \quad (4)$$

$$= Cs \times A \int_0^L \left[1 - erf\left(\frac{z}{2\sqrt{Dt}}\right)\right] dz$$

The *Cs* and *D* values were obtained by minimizing the above *obj* function.

3 RESULTS AND DISCUSSIONS

3.1 Diffusion of IL Enclosed in the ILRM

A snapshot from molecular dynamics simulation for the ILRM was shown in Figure 2. The [bmim][BF4] IL diffusion enclosed in the ILRM (Figure 2) was calciulated.

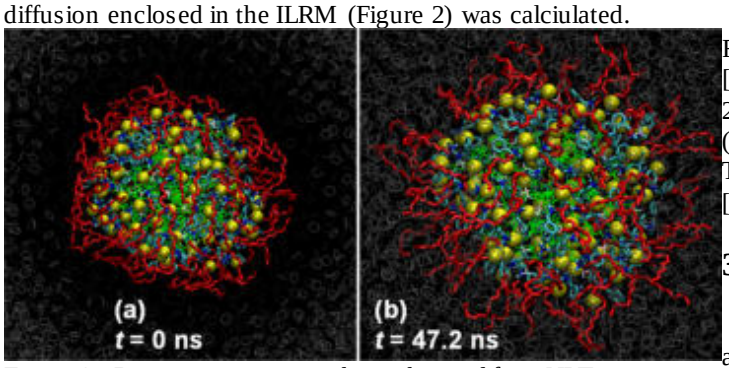

Figure 2. Representative snapshots obtained from NPT molecular dynamics simulations at 298 K and 1 bar. The ionic liquid reverse micelle (ILRM) system has 55798 atoms and contains 50 [bmim][BF_4] IL, 100 [BHDC] surfactant, and 7833 benzene molecules. The simulation was started (corresponding to time t = 0 ns) from a predefined ILRM nanodroplet (IL and surfactant) structure. Benzene molecules are indicated by gray sticks. [1]

The mean square displacement (MSD) (Figure 3) show that the $[bmim]^+$ cation and $[BF4]^-$ anion enclosed in the ILRM diffuse much faster than the neat [bmim][BF4] IL. Obtained from the MSD values, it was found that the self-diffusion coefficients for the [bmim][BF_4] IL enclosed in the ILRM diffuses about 16-35 times larger compared with the neat [bmim][BF_4] IL. The significantly enhanced IL self-diffusion in RM is partly due to the ILRM nanodroplet *particle* diffusion in less viscous benzene.

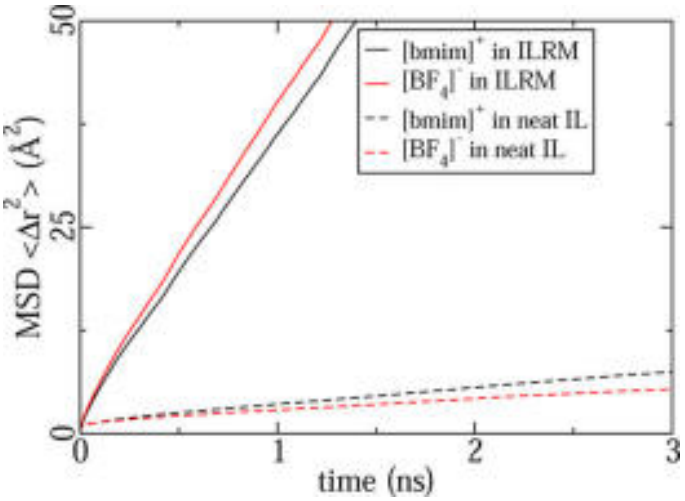

Figure 3. Mean squared displacement (MSD) for the [bmim]+ cation (black line) and [BF4]− anion (red line) at 298 K and 1 bar in the ionic liquid reverse micelle (ILRM) (solid line) and neat ionic liquid (IL) (dashed line) systems. The ILRM system consists of 50 [bmim][BF4] IL, 100 [BHDC], and 7833 benzene molecules [1].

3.2 CO_2 Absorption in ILRM

As shown in Figure 4, in the ILRM CO_2 could be absorbed in the benzene solvnet phase (IV), the intercae between benzene and the $[BHD]_+$ surfactant tail (III), $[BHD]_+$ surfactant tail (II), and inside the ILRM nanodroplet (I).

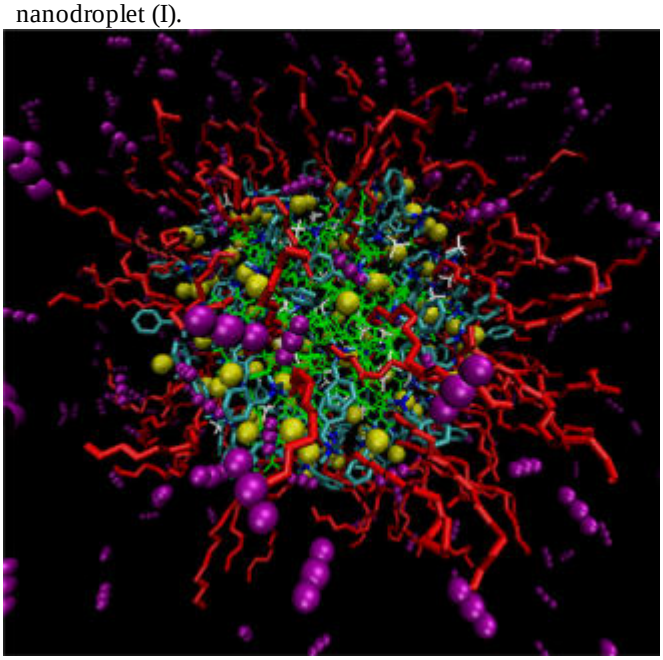

Figure 4. Representative snapshot for CO2 absorption in an ionic liquid reverse micelle (ILRM) system at 298 K and 1 bar. The ILRM system contains 50 [bmim][BF4] IL, 100 [BHDC] surfactant, and 7833 benzene molecules, in which 500 CO2 molecules are absorbed. The CO2 molecules are indicated as purple VDW. The IL and surfactant molecules

are represented in the same way as in Figure 2.Benzene solvent molecules are not shown for clarity [1].

CO_2 Henry's law constant, self-diffusivity and permeability were calculated (Table 1). The β values are close to 1, which suggest that the simulations are long enough to obtain reliable CO_2 self-duffusivity data. Note that the larger the Henry's law constant, the smaller gas solubility. The CO_2 solubility was found to decrease in the order II > III ~ IV > I, while the CO_2 diffusivity and permeability decrease in the following order: IV > III > II > I.

Table 1. Simulated CO_2 Henry's Law Constant (H), CO_2 Self-Diffusivity (D), and CO_2 Permeability (perm.) in Four Different Regions (Figure 4) of the Ionic Liquid Reverse Micelle (ILRM) System at 298 K[a] [1]

		self-diffusivity		
region	H (bar)	D (m^2/s)	β	perm. (barrer)
I	333.33	$9.1(5) \times 10^{-11}$	1.05(6)	76 ± 4
II	55.31	$3.4(1) \times 10^{-10}$	0.92(3)	1433 ± 42
III	89.29	$4.31(6) \times 10^{-9}$	0.91(2)	14300 ± 200
IV	88.90	$5.98(4) \times 10^{-9}$	0.97(1)	22270 ± 150

[a]The ILRM system contains 50 [bmim][BF_4]/100 [BHDC]/7833 C_6H_6. A total number of 500 CO_2 molecules are absorbed in the ILRM system. Note that the summation of cation and anion numbers rather than the number of IL pairs was used to compute the CO_2 molar fraction and Henry's law constant. The β = d(log Δr2)/d(log t) values obtained from simulations are also shown. The uncertainty in the last digit is given in parentheses.

3.3 CO_2 Diffusivity in Benzene, [bmim][BF_4] IL, and ILRM

The experimental CO_2 amounts of absorption in neat [bmim][BF_4] IL versus time are shown in Figure 5. The CO_2 Fickian diffusivity in [bmim][BF_4] at 298 K was calculated to be 1.146 $\times 10^{-10}$ m^2/s by fitting to the experimental data (Figure 5); which is comparable to the simulated CO_2 self-diffusivity of 9.9 ± 0.1 $\times 10^{-11}$ m^2/s [1] and the experimental data of 7.3 $\times 10^{-11}$ m^2/s obtained by Shiflett et al. The CO_2 Cs value was calculated to be 2.2393 mol/L by fitting to the experimental data. The fitted $N_{CO2}(t)$ values (Figure 5) are close to the experimental value, with an absolute average difference of 5.5%. The equilibrium amount of absorbed CO_2 was estimated to be 1.027 ± 0.001 mmol based on the experimental data at t > 26 hr (inset Figure 5), which corresponds to a CO_2 mole fraction of 0.188 at 13.059 ± 0.001 bar; this CO_2 equilibrium solubility data is comparable to the experimental data obtained by Shiflett et al. with a difference of about 10%.

Similarly, CO_2 diffusivity in benzene at 298 K was calculated to be 0.5-2 $\times 10^{-8}$ m^2/s, which is reasonably close to the simulation value of 0.6 $\times 10^{-8}$ m^2/s obtained from molecular dynamics simulations [1].

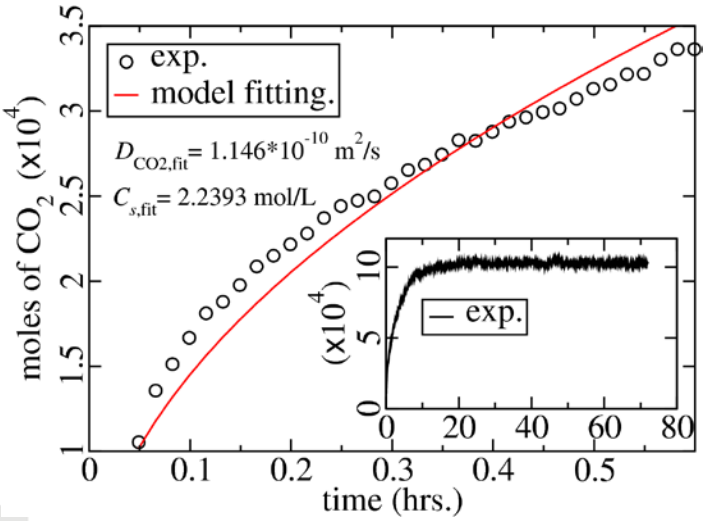

Figure 5. The experimental CO_2 amounts of absorption in [bmim][BF_4] ionic liquid versus time at 298 K during the initial time periods. Also shown are the calculated amounts of absorbed CO_2 versus time by using the $D_{CO2,\ fit}$ and $C_{s,\ fit}$ values. The experimental amounts of absorbed CO_2 in the whole time region are also shown in the inset of the figure.

For CO_2 absorption in the ILRM, the above fitting procedue by using equations (3-4) to obtain D and Cs does not work. There are large difference between the fitting and the experimental data; this is because the above equations (3-4) work only for a homogeneous solvent system and the diffusivity D is assumed to be a constant. However, in the ILRM CO_2 diffusivity values are very different from each other in different regions of the ILRM system (Table 1). In the ILRM system, if we assume that CO_2 diffusues three layers of benzene, the IL, and the surfactant in series, it takes about 10 times longer time than the experimental data. This is due to the large specifc area of the ILRM nanopartcile, in which CO2 diffuses into many ILRM nanopartciles parallely instead of serially.

.

REFERENCES

[1] W. Shi, L. Hong, K. Damodaran, H. B. Nulwala and D. R. Luebke, J. Phys. Chem. B, 118, 13870, 2014.